NMRlipids IV: Headgroup & glycerol backbone structures, and cation binding in bilayers with PE and PG lipids

O. H. Samuli Ollila[1, 2, *]

[1]*Institute of Organic Chemistry and Biochemistry, Academy of Sciences of the Czech Republic, Prague 6, Czech Republic*
[2]*Institute of Biotechnology, University of Helsinki*
(Dated: August 27, 2019)

Primarily measured but also simulated NMR order parameters will be collected also for other than phophatidylcholine (these are discussed in NMRlipids I) headgroup. The information will be used to understand structural differences between different lipid molecules in bilayers.

INTRODUCTION

In NMRlipids I and II project we were looking for a MD model which would correctly reproduce headgroup and glycerol backbone structures and cation binding for PC lipid bilayers [1, 2]. Here we extend the same goal for other than PC lipids. Currently the focus is on PE, PG and PS bilayers and their mixtures with PC. Experimental data with different amounts of added salt is now collected and presented in this manuscript.

Absolute values of experimental order parameters for different lipid headgroups are collected in Fig. 1. Signs are measured only for PC as far as I know, thus only absolute values are used for now.

Based on superficial reading, the conclusions in the literature are roughly
1) glycerol backbone structures are largely similar irrespectively of the headroup [3],
2) glycerol backbone and headgroup structure and behaviour are similar in model membranes and in bacteria [3–5],
3) headgroup structures are similar in PC, PE and PG lipids, while headgroup is more rigid in PS lipids [6, 7].
Extensive discussion about structural details of PE, PG or PS headgroups do not exists (as far as I know), In contrast to PC lipids (see [1] and references therein).

Several simulations containing PE, PG and PS lipids have been published [?], **1.List should be completed** however, glycerol backbone and headgroup order parameters are not compared to the experiments (based on superficial reading of literature).

METHODS

Experimental C–H bond order parameters

The headgroup and glycerol backbone C–H bond order parameter magnitudes and signs of POPE and POPG were determined by measuring the chemical-shift resolved dipolar splittings with a R-type Proton Detected Local Field (R-PDLF) experiment [8] and S-DROSS experiments [9] using natural abundance ^{13}C solid state NMR spectroscopy as described previously [10–12]. **2.The rest of the details to be written. I am not sure how much we need to repeat the NMRlipidsIVps paper.**

Molecular dynamics simulations

Molecular dynamics simulation data were collected using the Open Collaboration method [1], with the NMRlipids Project blog (nmrlipids.blogspot.fi) and GitHub repository (github.com/NMRlipids/NMRlipidsIVotherHGs) as the communication platforms. The simulated systems are listed in Tables I (pure PE and PG bilayers without additional ions). and III (mixtures and systems with additional ions). Further simulation details are given in the SI, and the simulation data are indexed in a searchable database available at www.nmrlipids.fi, and in the NMRlipids/MATCH repository (github.com/NMRlipids/MATCH).

The C–H bond order parameters were calculated directly from the carbon and hydrogen positions using the definition

$$S_{\mathrm{CH}} = \frac{1}{2}\langle 3\cos^2\theta - 1\rangle, \tag{1}$$

where θ is the angle between the C–H bond and the membrane normal (taken to align with z, with bilayer periodicity in the xy-plane). Angular brackets denote average over all sampled configurations. The order parameters were first calculated averaging over time separately for each lipid in the system. The average and the standard error of the mean were then calculated over different lipids. Python program (scripts/calcOrderParameters.py) that uses the MDAnalysis library [13, 14] is available in Ref. 15. The ion number density profiles were calculated using the gmx density tool of the Gromacs sofware package [16].

TABLE I: List of MD simulations with PE lipids.

lipid/counter-ions	force field for lipids / ions	NaCl (M)	^aN_l	^bN_w	^cN_c	^dT (K)	$^et_{sim}$(ns)	$^ft_{anal}$ (ns)	^{g}files
POPE	CHARMM36 [?]	0	144	5760	0	310	500	400	[17]
POPE	CHARMM36 [?]	0	500	25000	0	310	500	100	[18]
POPE	CHARMM36 [?]	0.11	500	25000	50	310	500	100	[19]
POPE	CHARMM36ua [?]	0	336	?	0	310	2×200	2×100	[20] 3.
DPPE	Slipids [21]	0	288	9386	0	336	200	100	[22]
POPE	Slipids [21?]	0	336	?	0	310	2×200	2×100	[23]
POPE	Slipids [?] 4.	0	500	25000	0	310	500	100	[24]
POPE	Slipids [?] 5.	0.11	500	25000	50	310	500	100	[25]
DPPE	GROMOS-CKP [?]	0	128	?	0	342	2×500	2×400	[26] 6.
POPE	GROMOS-CKP [?]	0	128	?	0	313	2×500	2×400	[27] 7.
POPE	GROMOS-CKP [?]	0	500	25000	0	310	500	100	[28]
DOPE	GROMOS-CKP [?]	0	128	?	0	271	2×500	2×400	[29] 8.
POPE	GROMOS 43A1-S3 [?]	0	128	?	0	313	2×200	2×100	[30] 9.
POPE	OPLS-UA vdW on H [?]	0	128	?	0	303	2×200	2×100	[31] 10.
POPE	OPLS-UA [?]	0	128	?	0	303	2×200	2×100	[32] 11.
POPE	Berger-based [?]	0	128	?	0	303	2×200	2×100	[33] 12.
POPE	Berger-based2 [?]	0	128	?	0	303	2×200	2×100	[34] 13.
DOPE	Berger-based [?]	0	128	?	0	271	2×200	2×100	[35] 14.
DOPE	Berger-based2 [?]	0	128	?	0	271	2×300	2×100	[36] 15.
POPE	LIPID17 [?]	0.11	500	25000	50	310	500	100	[37]

^{a}Number of lipid molecules with largest mole fraction
^{b}Number of water molecules
^{c}Number of additional cations
^{d}Simulation temperature
^{e}Total simulation time
^{f}Time used for analysis
^{g}Reference for simulation files

TABLE II: List of MD simulations with PG lipids.

lipid/counter-ions	force field for lipids / ions	NaCl (M)	^aN_l	^bN_w	^cN_c	^dT (K)	$^et_{sim}$(ns)	$^ft_{anal}$ (ns)	^{g}files
POPG/K^+	CHARMM36 [?] 16.	0	118	4110	0	298	100	100	[38]
POPG	CHARMM36 [?]	0.11	500	25000	49	310	500	100	[39]
POPG	CHARMM36 [?]	0	500	25000	0	310	500	100	[40]
POPG/Na^+	Slipids [41]	0	288	10664	0	298	250	100	[42]
DPPG/Na^+	Slipids [41]	0	288	11232	0	314	200	100	[43]
DPPG/Na^+	Slipids [41]	0	288	11232	0	298	400	100	[44]
POPG	Slipids [?] 17.	0	500	25000	0	310	500	100	[45]
POPG	Slipids [?] 18.	0.11	500	25000	49	310	500	100	[46]
POPG	LIPID17 [?]	0	500	25000	0	310	500	100	[47]
POPG	LIPID17 [?]	0.11	500	25000	49	310	500	100	[48]
POPG	GROMOS-CKP [?]	0	500	25000	0	310	500	100	[49]
POPG	GROMOS-CKP [?]	0.11	500	25000	0	310	500	100	[50]

^{a}Number of lipid molecules with largest mole fraction
^{b}Number of water molecules
^{c}Number of additional cations
^{d}Simulation temperature
^{e}Total simulation time
^{f}Time used for analysis
^{g}Reference for simulation files

TABLE III: List of MD simulations with PE and PG lipids mixed with PC.

lipid/counter-ions	force field for lipids / ions	NaCl (M)	CaCl$_2$ (M)	^{a}N$_l$	^{b}N$_w$	^{c}N$_c$	^{d}T (K)	^{e}t$_{sim}$(ns)	^{f}t$_{anal}$ (ns)	^{g}files
POPC	CHARMM36 [?]	0.11	0	500	25000	48	310	500	100	[51]
POPC:POPG (7:3)	CHARMM36 [?]	0.11	0	350	?	?	310	500	100	[52]
POPC:POPG (1:1)/K$^+$	CHARMM36 [?]	0	0	?	?	?	?	?	?	[?] 19.
POPC:POPG (1:1)/K$^+$	CHARMM36 [?]	0	0.15 20.	?	?	?	?	?	?	[?] 21.
POPC:POPG (1:1)/K$^+$	CHARMM36 [?]	0	1.0 22.	?	?	?	?	?	?	[?] 23.
POPC:POPG (4:1)/K$^+$	CHARMM36 [?]	0	0	?	?	?	?	?	?	[?] 24.
POPC:POPG (4:1)/K$^+$	CHARMM36 [?]	0	0.15 25.	?	?	?	?	?	?	[?] 26.
POPC:POPG (4:1)/K$^+$	CHARMM36 [?]	0	1.0 27.	?	?	?	?	?	?	[?] 28.
POPC	CHARMM36 [?]	0	0	256	8704	0	300	300	250	[53]
POPC:POPE (1:1)	CHARMM36 [?]	0	0	128	8704	0	300	300	250	[54]
POPC	Slipid [?]	0.11	0	500	25000	48	310	500	100	[55]
POPC:POPG (7:3)	Slipid [?]	?	0	?	?	?	310	500	100	[?] 29.
POPC	Berger [?] 30.	0	0	256	10240	0	300	300	200	[56]
POPC:POPE (1:1)	Berger [?] 31.	0	0	128	11008	0	300	300	200	[57]
POPC:DOPE (1:1)	Berger [?] 32.	0	0	128	10240	0	300	300	200	[58]
DOPC	Berger [?] 33.	0	0	256	11008	0	300	300	200	[59]
DOPC:DOPE (1:1)	Berger [?] 34.	0	0	128	11008	0	300	300	200	[60]

^{a}Number of lipid molecules with largest mole fraction
^{b}Number of water molecules
^{c}Number of additional cations
^{d}Simulation temperature
^{e}Total simulation time
^{f}Time used for analysis
^{g}Reference for simulation files

RESULTS AND DISCUSSION

Headgroup and glycerol backbone order parameters of POPE and POPG from ^{13}C NMR

The glycerol backbone and α-carbon peaks in INEPT spectra of POPE were assigned based on previously measured POPC spectra (Fig. S1) [10]. The β-carbon peak was assigned based on ^{13}C chemical shift table for amines available at `https://www.chem.wisc.edu/areas/reich/nmr/c13-data/cdata.htm`. The order parameters for the glycerol backbone and headgroup C–H bonds were determined from 2D-RPDLF and S-DROSS experiments (Fig. S1), as described previously [12]. The POPE experiments were recorded at 310 K, where the bilayer is in liquid disordered phase [?]. **35.Details to be checked by Tiago.**

36.Figure and discussion about POPG experiments to be addded.

The headgroup and glycerol backbone order parameters of PE lipids are similar with different acyl chains and also close the values for POPC, althought PE gives systematically slightly more positive values (Fig. 1). These could be explained with slightly larger temperature in PE measurements, except for the α-carbon with the positive sign, for which the more positive value is farther away from zero. For PG lipids, the glycerol backbone order parameters are more positive than for other lipids. The headgroup α-carbon gives value close to PE, while the value of β-carbon is distinct from other lipid being only one which has positive sign, suggesting distinct conformation of PG lipids in this region. This was not observed in previous ^{2}H NMR study, where sign was not measured and β-carbon order parameter was apparently similar to the value for PE and PC results.

In conclusion, the results suggests that the glycerol backbone conformations in all lipids are relatively similar. Also, the headgroup conformations are similar for PC and PE lipids, while PS and PG are singnificantly different. For PS lipids, the differences are discussed previously [?].

Headgroup and glycerol backbone of POPE and POPG in MD simulations

The glycerol backbone order parameters in Slipid simulations are off from experiments for both PE and PG lipids (Figs. 2 and 3), as already reported previously for PC lipids [1] and PS lipids [12]. The Slipid simulations were able to capture the essential differences between PC and PS lipid headgroups [12], but this is not the case for PE and PG lipids.

38.Berger results are not here yet, but we should mention the ring like structures pointed out by T. Piggot in the blog: The poor performance of headgroup order parameters in Berger model can be probably explained by ring like structures seen in Fig. 6 in Ref. 64. These ring like structures are a widespread feature of typical Berger based lipid force fields containing explicit hydrogen atoms in the head group [65–67].

CHARMM36 simulations seems to capture all the essential differences between headgroup order parameters of PC PE,
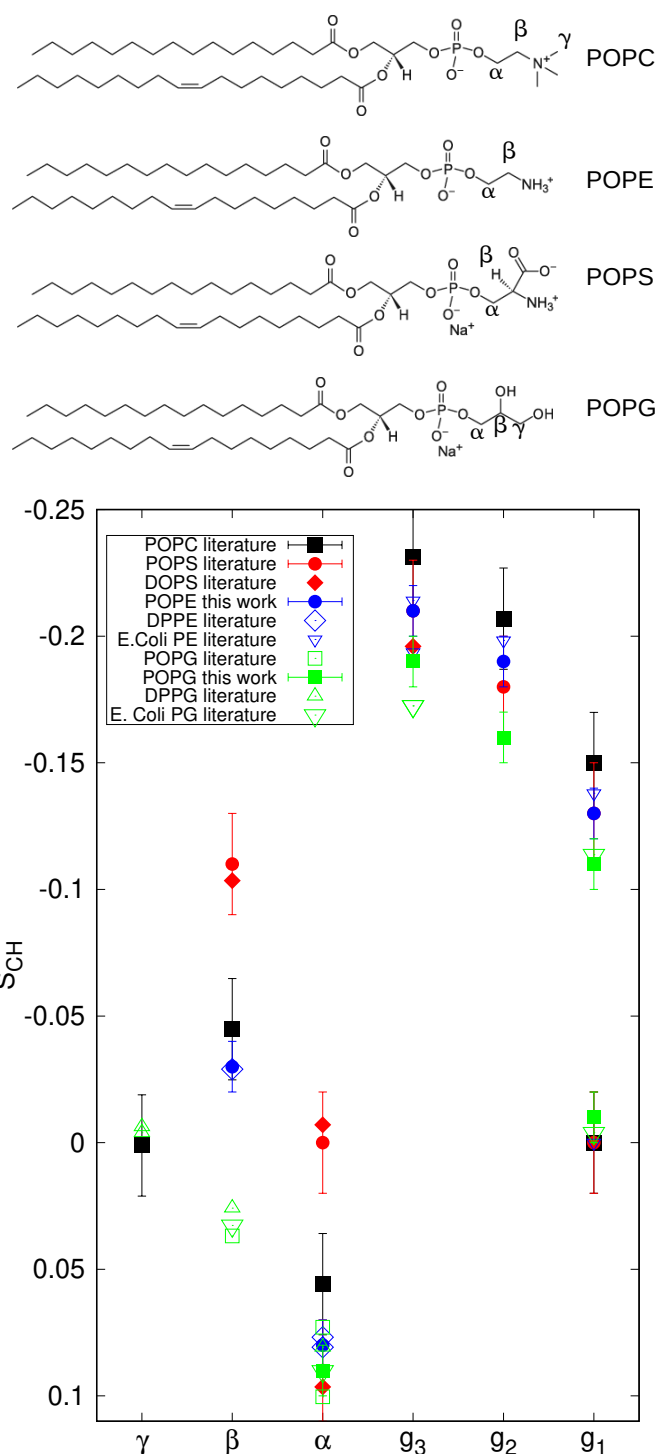

FIG. 1: (top) Chemical structure of different lipids (bottom) Headgroup and glycerol backbone order parameters measured from lipids with different headgroups in lamellar liquid disordered phase. The values and signs for POPE (310 K), POPG (298 K). POPS (298 K) [12] and POPC (300 K) [10, 11] are measured using ^{13}C NMR. The literature values for DOPS with 0.1M of NaCl (303 K) [61], POPG with 10nM PIPES (298 K) [62], DPPG with 10mM PIPES and 100mM NaCl (314 K) [6], DPPE (341 K) [63], E.coliPE and E.coliPG (310 K) [3] are measured using ^{2}H NMR. The signs from ^{13}C NMR are used also for the literature values.
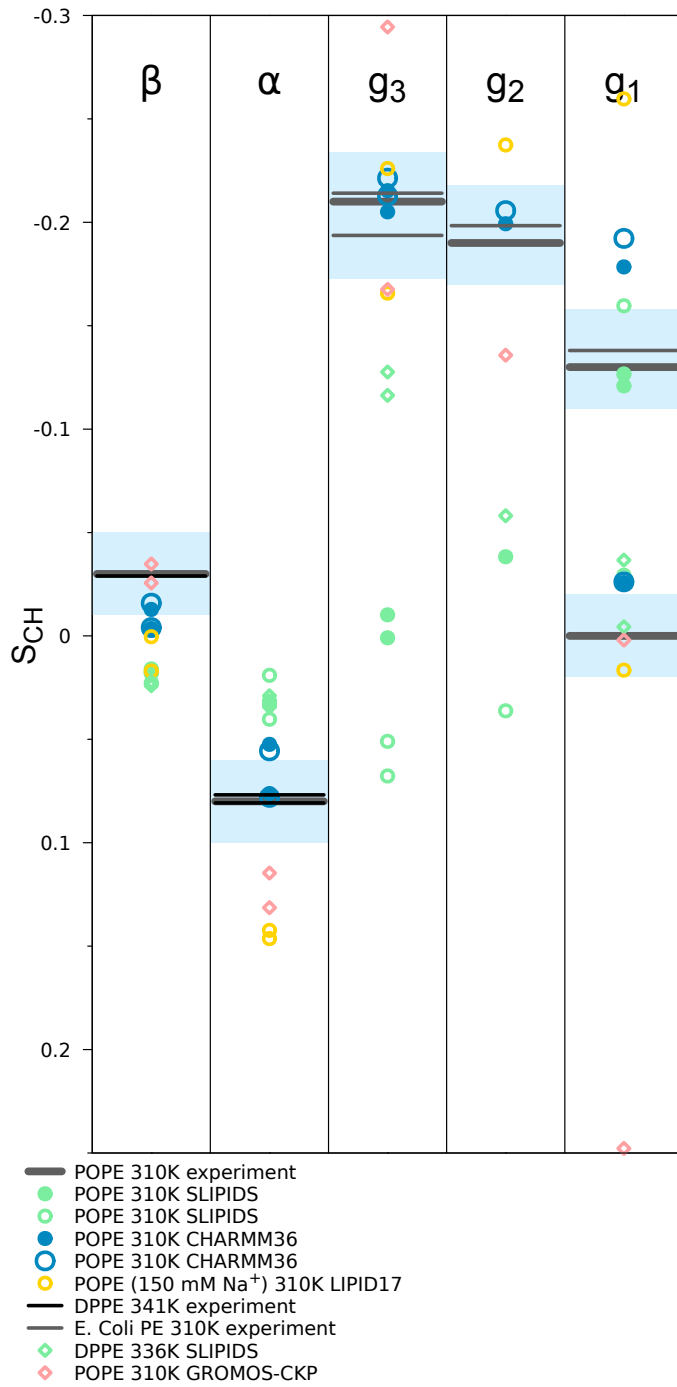
FIG. 2: The headgroup and glycerol backbone order parameters of PE lipids from experiments (POPE and signs this work, DPPE from Ref. 63 and E.coliPE from Ref. 3) and simulations with different force fields.

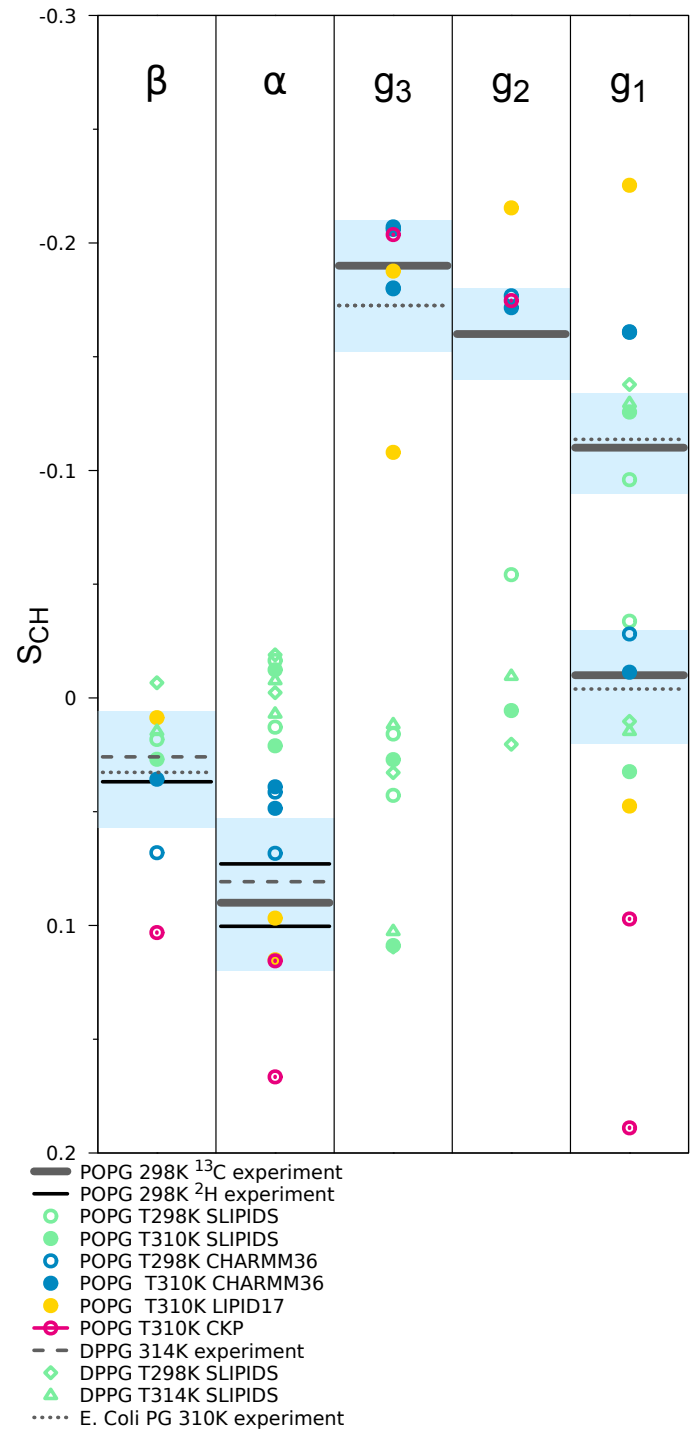**37.Results from united atom GROMOS,CHARMM36ua,OPLS-UA,Berger and GROMOS-CKP simulations yet to be analyzed and added**

FIG. 3: The headgroup and glycerol backbone order parameters of PG lipids from experiments (POPG and signs from this work and from Ref. 62, DPPG with 100mM NaCl from Ref. 6,and E.Coli PG results from Ref. 3). and simulations with different force fields.

PG (Figs. 2 and 3), as previously observed also for PS lipids [12]. Therefore, the CHARMM36 simulations can be used to analyze the structural differences between headgroups **39.We should do such analysis. Maybe similar to the PS part [12]?**

Lipid headgroup interactions in PC:PE and PC:PG mixtures

According to the electrometer concept, the headgroup order parameters increase with the addition of negatively charged PG lipids, but are not affected by the addition of zwitterionic PE lipids (Fig. 4) [4, 68]. This is roughly observed also in simulations here, althouht the changes in PC headgroup with PE are slightly overestimated and changes with PG lipid are slightly underestimated. The underestimated increase of PC headgroup order parameters with the addition of negaticely charged lipids was previously interepreted to indicate overestimated counterion binding affinity, which overcompensates the effect of negative charge [12]. Thus, the counterion binding to PG lipid bilayers (Fig. 5) may be slightly overestimated also in simulations here.

41.This is text by P. Fuchs, copied from the blog.

Area results in nm^2, the error is $<= 0.003$ nm^2

- pure POPC

CHARMM36: 0.624

Berger : 0.649

- POPC/POPE 50:50

CHARMM36 : POPC 0.609, POPE 0.557

Berger-hacked: POPC 0.637, POPE 0.632

——

One can see that CHARMM 36 predicts a drop in the area on going from pure POPC to POPC/POPE 50:50. This means that POPC pack tightly to POPE. In contrast, the values for Berger are not that changed. The POPE value predicted by CHARMM 36 (in the mixture POPC/POPE 50:50) is much smaller than that predicted by Berger.

——-

The experimental acyl chain order parameters for POPE [71] seem larger than reported for POPC [10], which supports the more condensed PE bilayer. In principle, this is beyond the scope of this work (lipid headgroups), but we can consider mentioning this.

The order parameter of headgroup β-carbon of PG slightly increases with the addition of PC [69], although also smaller changes have been observed [62] (Fig. **??**). The increase in PG headgroup order parameter is not observed in simulations, which may arise from overestimated counterion binding overcompensating the changes in electrostatic environment as suggested for PC headgroup above. However, the changes are quite small and not fully consistent in experiments.
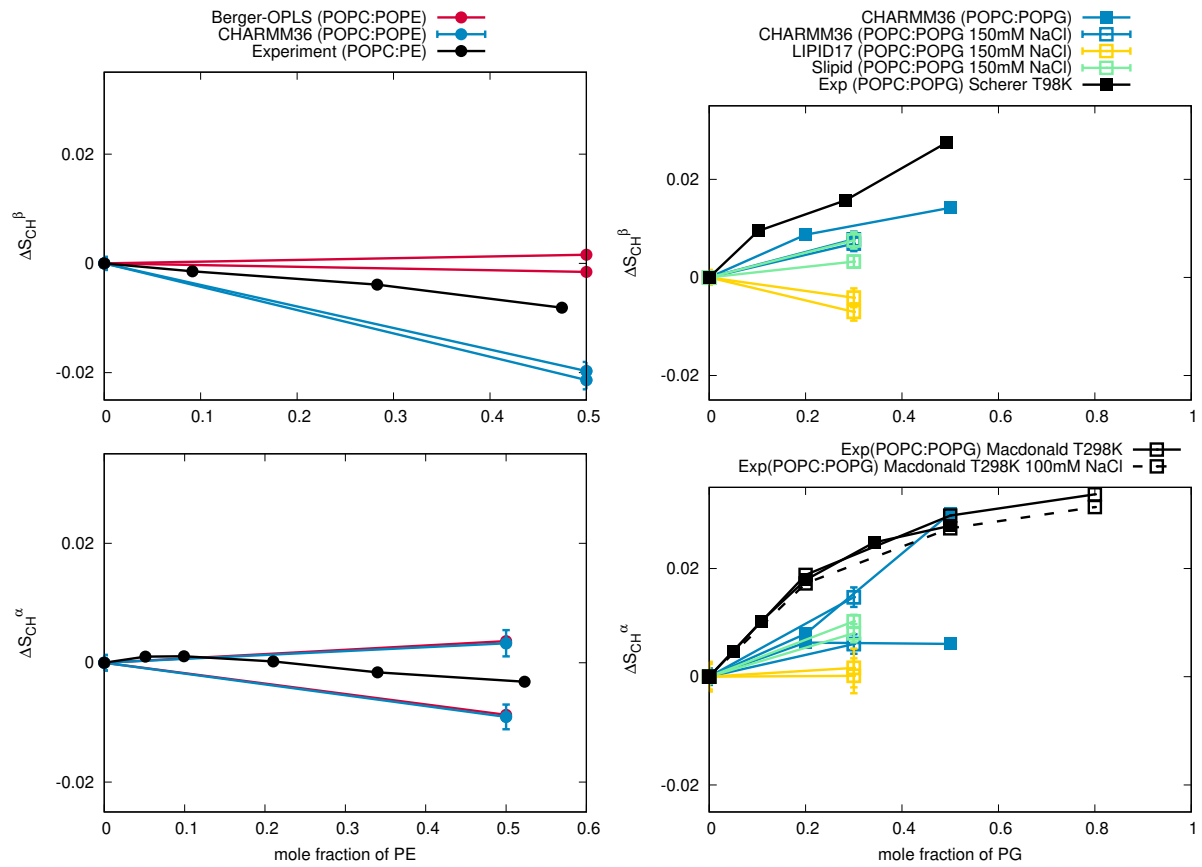
FIG. 4: Modulation of PC headgroup order parameters with increasing amount of PE (left) and PG (right) in bilayer from experiments [4, 69] and simulations with different force fields. Signs are determined as discussed in [1, 70].

40.Simulation of CHARMM36 at 298K should be maybe rerun with Gromacs 5.
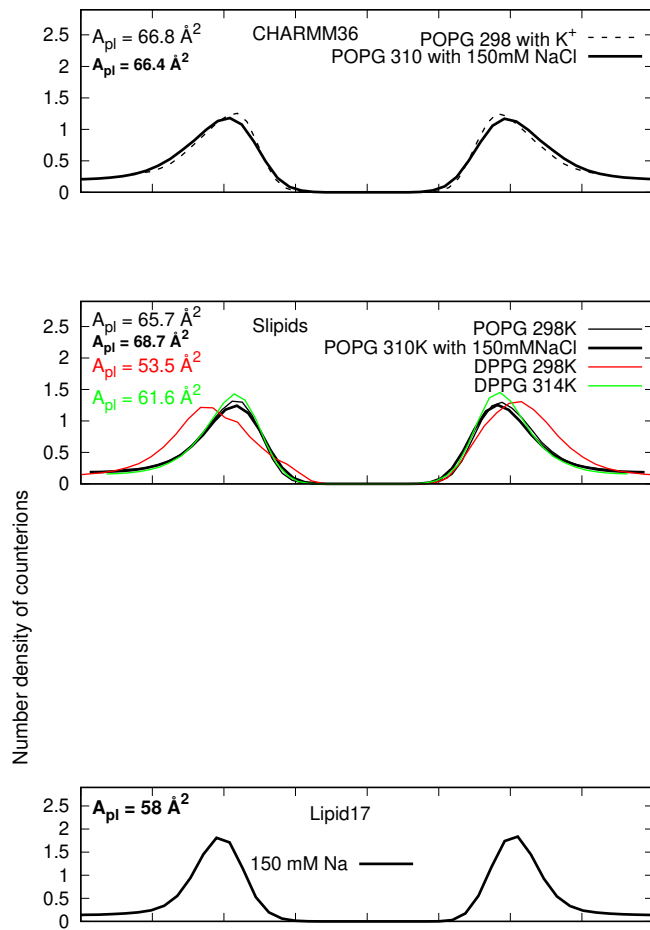
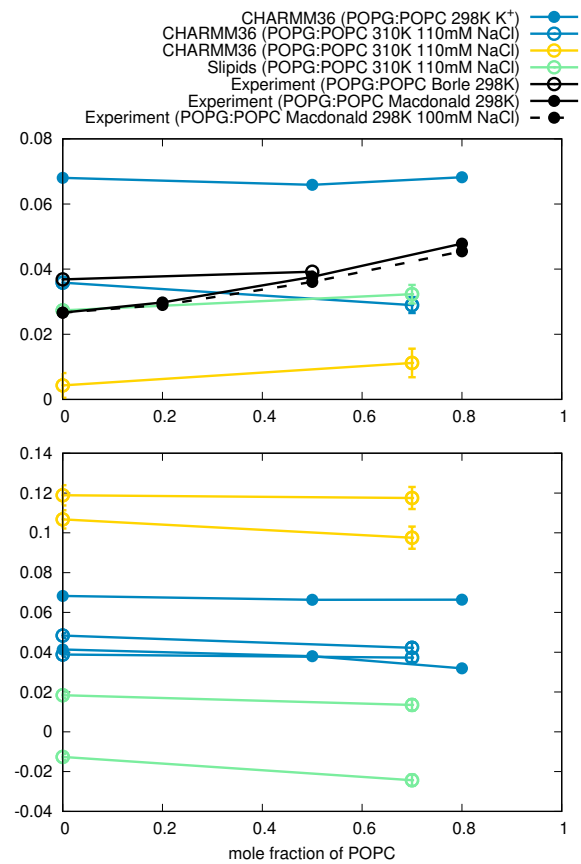FIG. 5: Counterion densities from simulations with PG lipids.

FIG. 6: Modulation of PG lipid headgroup order parameters with the increasing amount of PC in lipid bilayer from experiments [62, 69] and simulations with different force fields.

Cation binding to PE and PG lipid bilayers

The headgroup order parameters of PC lipids can used to measure ion binding affinity to lipid bilayers, because their magnitude is linearly proportional to the amount of bound charge in bilayer according to the molecular electrometer concept [2, 68]. The molecular electrometer concept can be used also for bilayers containing PC lipids mixed with charged lipids [12, 62, 69, 72]. Based on the electrometer concept and other data is has been suggested that [5]

> "(i) Ca^{2+} binds to neutral lipids (phosphatidyl-choline, phosphatidylethanolamine) and negatively charged lipids (phosphatidylglycerol) with approximately the same binding constant of $K = 10$-$20\ M^{-1}$;
> (ii) the free Ca^{2+} concentration at the membrane interface is distinctly enhanced if the membrane carries a negative surface charge, either due to protein or to lipid;
> (iii) increased inter-facial Ca^{2+} also means increased amounts of bound Ca^{2+} at neutral and charged lipids;
> (iv) the actual binding step can be described by a Langmuir adsorption isotherm with a 1 lipid:1 Ca^{2+} stoichiometry, provided the interfacial concentration C_M, is used to describe the chemical binding equilibrium."

The electrometer concept has been very useful in evaluating ion binding affinity in simulations against experiments, because the headgroup order parameter changes as a function of ion concentration can be directly compared with experiments [2, 12, 73].

Sodium binding to PC lipid bilayers is significantly overestimated by most simulations models [2]. Also, sodium binding to PS lipids seems to be overestimated, although the presence of counterions complicate the comparison for negatively charged lipids [12]. Sodium binding to PE lipids is weaker than to PC lipids in previous work [2] in both CHARMM36 and Slipids simulations (Fig. 7). This cannot be evaluated using electrometer concept because experimental data with PE lipids is not available **42.Other experimental data should be checked and discussed**. The difference in Slipids may also be due to different ion model used **43.The used ion model here should be checked**.

Calcium binding affinity to PC and PS lipid bilayers was not correctly described by any of the standard MD simulation forced fields [2, 12], while recently introduced force field with electronic continuum correction (ECC) performed better [73]. The decrease of α-carbon order parameter of PC lipids in PC:PG mixtures as a function of calcium concentration is close to experiments CHARMM36 simulations (Fig. 8), but the decrease of β-carbon order parameter seems to be overestimated. However, the β-carbon order parameter was not actually measured from these samples, but they are calculated from empirical relation $\Delta S_\beta = 0.43\Delta S_\alpha$ [74]. The result is
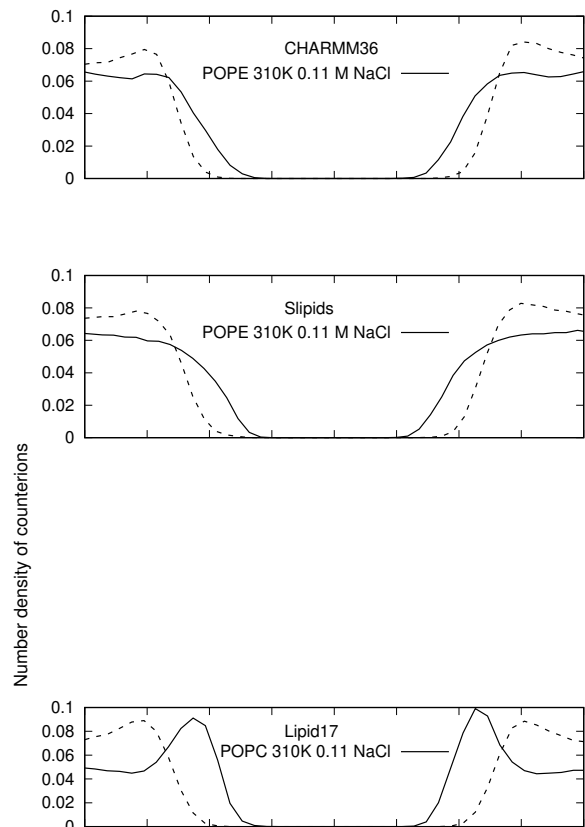

FIG. 7: Sodium (solid line) and choride ion density profiles along membrane normal from different simulations with PE lipids.

similar to the $\sim$200 ns simulations with PC lipids in previous work [2]. However, when simulation was continued for μs, the binding affinity substantially increased and interpretation was that calcium overbinds to PC lipid in CHARMM36. Therefore, the conclusion seems to be similar here, although the new NBfix parameters may complicate the situation **44.The status of NBfix parameters in these simulations should be checked.**.

The β-carbon order parameter of PG exhibits a rapid decrease with small $CaCl_2$ concentrations and a more modest decrease with larger concentrations in experiments [62] (Fig. **??**). The rapid decrease with $CaCl_2$ is observed but overestimated in CHARMM36 simulation with POPC:POPG 1:1 mixture, but not in 4:1 mixture **45.This is little bit weird, should be checked.**.

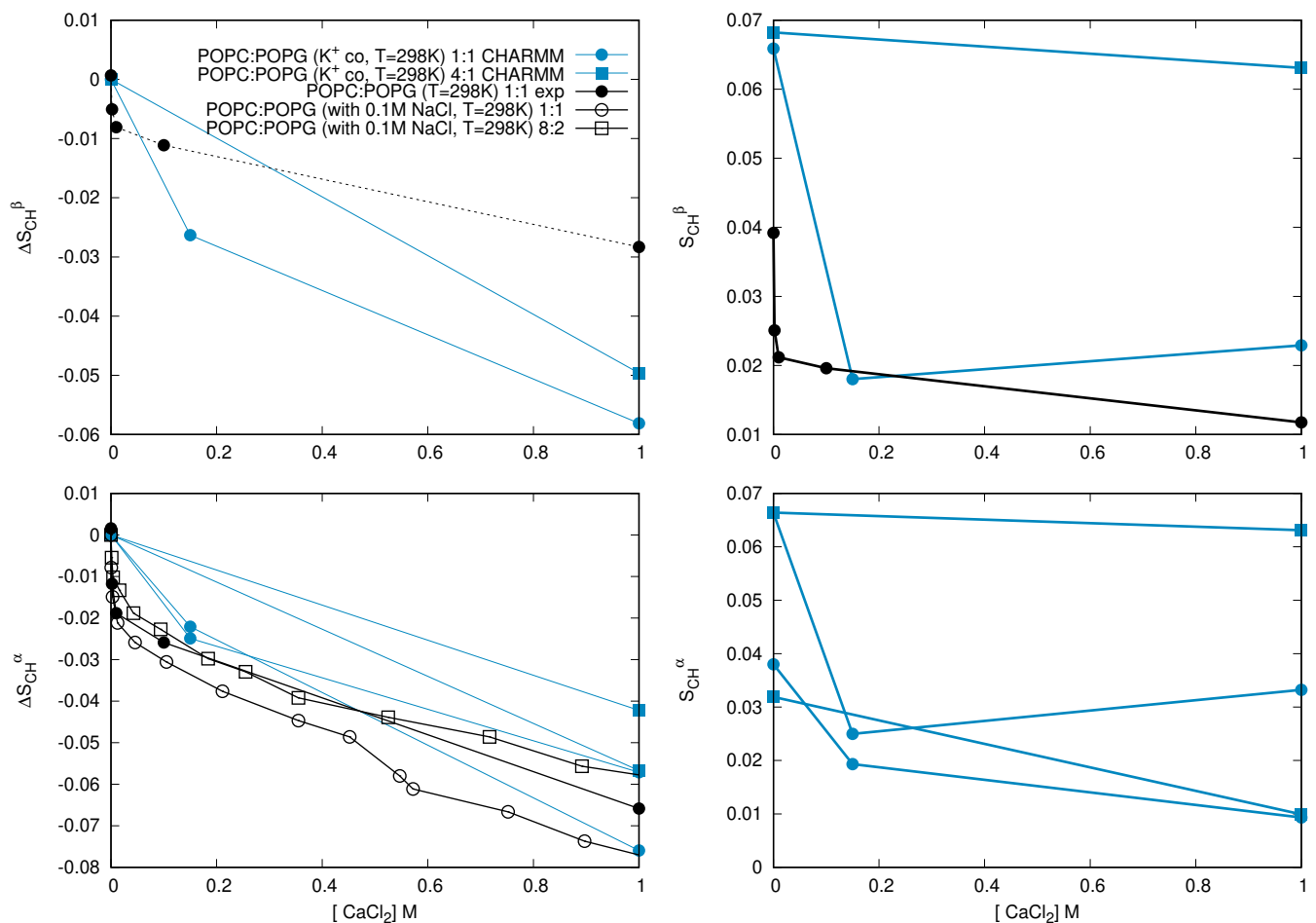**46.We need PC:PG simulations with $CaCl_2$ from different force fields to finish the discussion.**

FIG. 8: (left) The headgroup order parameters of PC from PC:PG mixtures as a function CaCl$_2$ concentration from experiments [62, 69] and CHARMM36 simulations. Note that beta order parameter is calculated from empirical relation $\Delta S_\beta = 0.43 \Delta S_\alpha$ [74], not actually measured. (right) The headgroup order parameters of PG from PC:PG mixtures as a function CaCl$_2$ concentration from experiments [62] and CHARMM36 simulations.

CONCLUSIONS

SUPPLEMENTARY INFORMATION

* samuli.ollila@helsinki.fi

[1] A. Botan, F. Favela-Rosales, P. F. J. Fuchs, M. Javanainen, M. Kanduč, W. Kulig, A. Lamberg, C. Loison, A. Lyubartsev, M. S. Miettinen, et al., J. Phys. Chem. B **119**, 15075 (2015).

[2] A. Catte, M. Girych, M. Javanainen, C. Loison, J. Melcr, M. S. Miettinen, L. Monticelli, J. Maatta, V. S. Oganesyan, O. H. S. Ollila, et al., Phys. Chem. Chem. Phys. **18**, 32560 (2016).

[3] H. U. Gally, G. Pluschke, P. Overath, and J. Seelig, Biochemistry **20**, 1826 (1981).

[4] P. Scherer and J. Seelig, EMBO J. **6** (1987).

[5] J. Seelig, Cell Biology International Reports **14**, 353 (1990), ISSN 0309-1651, URL http://www.sciencedirect.com/science/article/pii/030916519091204H.

[6] R. Wohlgemuth, N. Waespe-Sarcevic, and J. Seelig, Biochemistry **19**, 3315 (1980).
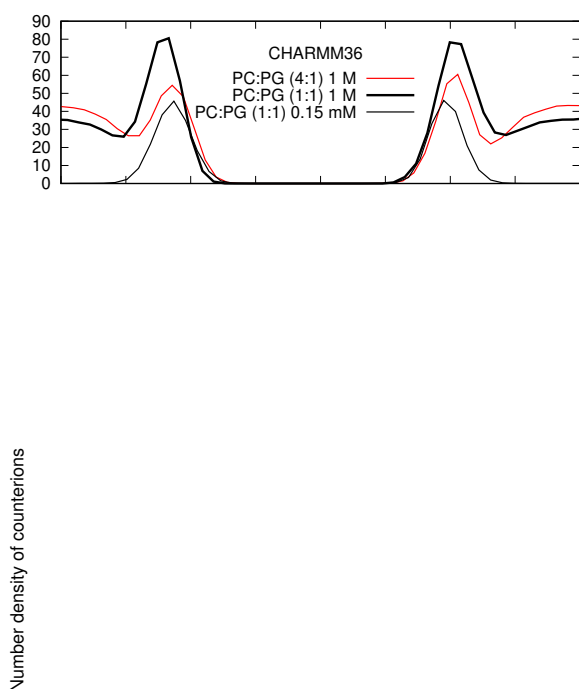
FIG. 9: Calcium ion density profiles along membrane normal from different simulations with PG lipids.

[7] G. Büldt and R. Wohlgemuth, The Journal of Membrane Biology **58**, 81 (1981), ISSN 1432-1424, URL http://dx.doi.org/10.1007/BF01870972.

[8] S. V. Dvinskikh, H. Zimmermann, A. Maliniak, and D. Sandstrom, J. Magn. Reson. **168**, 194 (2004).

[9] J. D. Gross, D. E. Warschawski, and R. G. Griffin, J. Am. Chem. Soc. **119**, 796 (1997).

[10] T. M. Ferreira, F. Coreta-Gomes, O. H. S. Ollila, M. J. Moreno, W. L. C. Vaz, and D. Topgaard, Phys. Chem. Chem. Phys. **15**, 1976 (2013).

[11] T. M. Ferreira, R. Sood, R. Bärenwald, G. Carlström, D. Topgaard, K. Saalwächter, P. K. J. Kinnunen, and O. H. S. Ollila, Langmuir **32**, 6524 (2016).

[12] H. Antila, P. Buslaev, F. Favela, T. M. Ferreira, I. Gushchin, M. Javanainen, B. Kav, J. J. Madsen, J. Melcr, M. Miettinen, et al., *Nmrlipids iv: Headgroup & glycerol backbone structures, and cation binding in bilayers with ps lipids* (2019), URL https://github.com/NMRLipids/NMRlipidsIVotherHGs/blob/master/Manuscript/manuscriptPS.pdf.

[13] N. Michaud-Agrawal, E. J. Denning, T. B. Woolf, and O. Beckstein, Journal of Computational Chemistry **32**, 2319 (2011), https://onlinelibrary.wiley.com/doi/pdf/10.1002/jcc.21787, URL https://onlinelibrary.wiley.com/doi/abs/10.1002/jcc.21787.

[14] Richard J. Gowers, Max Linke, Jonathan Barnoud, Tyler J. E. Reddy, Manuel N. Melo, Sean L. Seyler, Jan Domański, David L. Dotson, Sébastien Buchoux, Ian M. Kenney, et al., in *Proceedings of the 15th Python in Science Conference*, edited by Sebastian Benthall and Scott Rostrup (2016), pp. 98 – 105.

[15] ohsOllila and et al., *Match github repository*, URL https://github.com/NMRLipids/MATCH.

[16] M. Abraham, D. van der Spoel, E. Lindahl, B. Hess, and the GROMACS development team, *GROMACS user manual version 5.0.7* (2015), URL www.gromacs.org.

[17] M. Javanainen, *Simulation of a POPE bilayer at 310K with the CHARMM36 force field* (2019), URL https://doi.org/10.5281/zenodo.2641987.

[18] PEON, *CHARMM36 POPE Bilayer Simulation (Last 100 ns, 310 K)* (2019), URL https://doi.org/10.5281/zenodo.3237461.

[19] A. PEÓN, *CHARMM36 POPE Bilayer Simulation (Last 100 ns, 150 mM NaCl, 310 K)* (2019), URL https://doi.org/10.5281/zenodo.2577454.

[20] T. Piggot, *CHARMM36-UA POPE Simulations (versions 1 and 2) 310 K (NOTE: hexagonal membrane and POPE is called PEUA)* (2018), URL https://doi.org/10.5281/zenodo.1293774.

[21] J. P. M. Jämbeck and A. P. Lyubartsev, J. Chem. Theory Comput. **8**, 2938 (2012).

[22] F. Favela-Rosales, *MD simulation trajectory of a fully hydrated DPPE bilayer: SLIPIDS, Gromacs 5.0.4. 2017.* (2017), URL https://doi.org/10.5281/zenodo.495247.

[23] T. Piggot, *Slipids POPE Simulations (versions 1 and 2) 310 K (NOTE: hexagonal membrane)* (2018), URL https://doi.org/10.5281/zenodo.1293813.

[24] A. Peon, *SLIPID POPE Bilayer Simulation (Last 100 ns, 310 K)* (2019), URL https://doi.org/10.5281/zenodo.3231342.

[25] A. PEÓN, *SLIPID POPE Bilayer Simulation (Last 100 ns, 150 mM NaCl, 310 K)* (2019), URL https://doi.org/10.5281/zenodo.2578069.

[26] T. Piggot, *GROMOS-CKP DPPE Simulations (versions 1 and 2) 342 K* (2018), URL https://doi.org/10.5281/zenodo.1293957.

[27] T. Piggot, *GROMOS-CKP POPE Simulations (versions 1 and 2) 313 K* (2018), URL https://doi.org/10.5281/zenodo.1293932.

[28] A. PEON, *GROMOS POPE Bilayer Simulation (Last 100 ns, 310 K)* (2019), URL https://doi.org/10.5281/zenodo.3237754.

[29] T. Piggot, *GROMOS-CKP DOPE Simulations (versions 1 and 2) 271 K* (2018), URL https://doi.org/10.5281/zenodo.1293941.

[30] T. Piggot, *GROMOS 43A1-S3 POPE Simulations (versions 1 and 2) 313 K (NOTE: anisotropic pressure coupling)* (2018), URL https://doi.org/10.5281/zenodo.1293762.

[31] T. Piggot, *OPLS-UA POPE Simulations (versions 1 and 2) 303 K with vdW on H atoms* (2018), URL https://doi.org/10.5281/zenodo.1293853.

[32] T. Piggot, *Opls-ua pope simulations (versions 1 and 2) 303*

k (2018), URL https://doi.org/10.5281/zenodo.1293855.

[33] T. Piggot, *Berger POPE Simulations (versions 1 and 2) 303 K - de Vries repulsive H* (2018), URL https://doi.org/10.5281/zenodo.1293889.

[34] T. Piggot, *Berger POPE Simulations (versions 1 and 2) 303 K - larger repulsive H* (2018), URL https://doi.org/10.5281/zenodo.1293891.

[35] T. Piggot, *Berger DOPE Simulations (versions 1 and 2) 271 K - de Vries repulsive H* (2018), URL https://doi.org/10.5281/zenodo.1293928.

[36] T. Piggot, *Berger DOPE Simulations (versions 1 and 2) 271 K - larger repulsive H* (2018), URL https://doi.org/10.5281/zenodo.1293905.

[37] A. PEÓN, *LIPID17 POPE Bilayer Simulation (Last 100 ns, 150 mM NaCl, 310 K)* (2019), URL https://doi.org/10.5281/zenodo.2577305.

[38] O. H. S. Ollila, *POPG lipid bilayer simulation at T298K ran with MODEL_CHARMM_GUI force field and Gromacs* (2017), URL https://doi.org/10.5281/zenodo.1011096.

[39] A. PEÓN, *CHARMM36 POPG Bilayer Simulation (Last 100 ns, 150 mM NaCl, 310 K)* (2019), URL https://doi.org/10.5281/zenodo.2573531.

[40] ANTONIO, *CHARMM36 POPG Bilayer Simulation (Last 100 ns, 310 K)* (2019), URL https://doi.org/10.5281/zenodo.3237463.

[41] J. P. M. Jämbeck and A. P. Lyubartsev, Phys. Chem. Chem. Phys. **15**, 4677 (2013).

[42] F. Favela-Rosales, *MD simulation trajectory of a fully hydrated POPG bilayer: SLIPIDS, Gromacs 5.0.4. 2017.* (2017), URL https://doi.org/10.5281/zenodo.546133.

[43] F. Favela-Rosales, *MD simulation trajectory of a fully hydrated DPPG bilayer @314K: SLIPIDS, Gromacs 5.0.4. 2017.* (2017), URL https://doi.org/10.5281/zenodo.546136.

[44] F. Favela-Rosales, *MD simulation trajectory of a fully hydrated DPPG bilayer @298K: SLIPIDS, Gromacs 5.0.4. 2017.* (2017), URL https://doi.org/10.5281/zenodo.546135.

[45] A. PEÓN, *SLIPID POPG Bilayer Simulation (Last 100 ns, 310 K)* (2019), URL https://doi.org/10.5281/zenodo.3364460.

[46] A. PEÓN, *SLIPID POPG Bilayer Simulation (Last 100 ns, 150 mM NaCl, 310 K)* (2019), URL https://doi.org/10.5281/zenodo.2633773.

[47] A. PEON, *LIPID17 POPG Bilayer Simulation (Last 100 ns, 310 K)* (2019), URL https://doi.org/10.5281/zenodo.3247659.

[48] A. PEÓN, *LIPID17 POPG Bilayer Simulation (Last 100 ns, 150 mM NaCl, 310 K)* (2019), URL https://doi.org/10.5281/zenodo.2573905.

[49] A. PEON, *GROMOS POPG Bilayer Simulation (Last 100 ns, 310 K)* (2019), URL https://doi.org/10.5281/zenodo.3266166.

[50] A. PEÓN, *Gromos POPG Bilayer Simulation (Last 100 ns, 150 mM NaCl, 310 K)* (2019), URL https://doi.org/10.5281/zenodo.3257649.

[51] A. Peón, *CHARMM36 POPC Bilayer Simulation (Last 100 ns, 150 mM NaCl, 310 K)* (2019), URL https://doi.org/10.5281/zenodo.2628335.

[52] A. PEÓN, *CHARMM36 POPC-POPG 7:3 Bilayer Simulation (Last 100 ns, 150 mM NaCl, 310 K)* (2019), URL https://doi.org/10.5281/zenodo.2580902.

[53] C. Papadopoulos and P. F. Fuchs, *CHARMM36 pure POPC MD simulation (300 K - 300ns - 1 bar)* (2018), URL https://doi.org/10.5281/zenodo.1306800.

[54] C. Papadopoulos and P. F. Fuchs, *CHARMM36 POPC/POPE (50%-50%) MD simulation (300 K - 300ns - 1 bar)* (2018), URL https://doi.org/10.5281/zenodo.1306821.

[55] A. PEÓN, *SLIPID POPC Bilayer Simulation (Last 100 ns, 150 mM NaCl, 310 K)* (2019), URL https://doi.org/10.5281/zenodo.2574689.

[56] B. Amélie and F. P. F.J., *Berger pure POPC MD simulation (300 K - 300ns - 1 bar)* (2018), URL https://doi.org/10.5281/zenodo.1402417.

[57] B. Amélie and F. P. F.J., *Berger POPC/POPE (50:50 ratio) MD simulation (300 K - 400ns - 1 bar)* (2018), URL https://doi.org/10.5281/zenodo.1402449.

[58] B. Amélie and F. P. F.J., *Berger POPC/DOPE (50:50 ratio) MD simulation (300 K - 300ns - 1 bar)* (2018), URL https://doi.org/10.5281/zenodo.1402441.

[59] B. Amélie and F. P. F.J., *Berger pure DOPC MD simulation (300 K - 300ns - 1 bar)* (2018), URL https://doi.org/10.5281/zenodo.1402411.

[60] B. Amélie and F. P. F.J., *Berger DOPC/DOPE (50:50 ratio) MD simulation (300 K - 300ns - 1 bar)* (2018), URL https://doi.org/10.5281/zenodo.1402437.

[61] J. L. Browning and J. Seelig, Biochemistry **19**, 1262 (1980).

[62] F. Borle and J. Seelig, Chemistry and Physics of Lipids **36**, 263 (1985).

[63] J. Seelig and H. U. Gally, Biochemistry **15**, 5199 (1976).

[64] P. Mukhopadhyay, L. Monticelli, and D. P. Tieleman, Biophysical Journal **86**, 1601 (2004).

[65] W. Zhao, T. Róg, A. A. Gurtovenko, I. Vattulainen, and M. Karttunen, Biochimie **90**, 930 (2008), ISSN 0300-9084, URL http://www.sciencedirect.com/science/article/pii/S0300908408000692.

[66] J. Hénin, W. Shinoda, and M. L. Klein, The Journal of Physical Chemistry B **113**, 6958 (2009).

[67] M. Dahlberg, A. Marini, B. Mennucci, and A. Maliniak, The Journal of Physical Chemistry A **114**, 4375 (2010).

[68] J. Seelig, P. M. MacDonald, and P. G. Scherer, Biochemistry **26**, 7535 (1987).

[69] P. M. Macdonald and J. Seelig, Biochemistry **26**, 1231 (1987).

[70] O. S. Ollila and G. Pabst, Biochimica et Biophysica Acta (BBA) - Biomembranes **1858**, 2512 (2016).

[71] C. Paré and M. Lafleur, Biophysical Journal **74**, 899 (1998), ISSN 0006-3495, URL http://www.sciencedirect.com/science/article/pii/S0006349598740135.

[72] M. Roux and M. Bloom, Biochemistry **29**, 7077 (1990).

[73] J. Melcr, H. Martinez-Seara, R. Nencini, J. Kolafa, P. Jungwirth, and O. H. S. Ollila, The Journal of Physical Chemistry B **122**, 4546 (2018).

[74] H. Akutsu and J. Seelig, Biochemistry **20**, 7366 (1981).

ToDo